Air-sea exchange and gas-particle partitioning of polycyclic aromatic hydrocarbons in the Mediterranean

Marie D. Mulder[a], Angelika Heil[b], Petr Kukučka[a], Jana Klánová[a], Jan Kuta[a], Roman Prokeš[a], Francesca Sprovieri[c], Gerhard Lammel[a,d*]

[a] Masaryk University, Research Centre for Toxic Compounds in the Environment, Brno, Czech Republic

[b] Helmholtz Research Centre Jülich, Institute for Energy & Climate Research, Jülich, Germany

[c] CNR, Institute for Atmospheric Pollution Research, Rende, Italy

[d] Max Planck Institute for Chemistry, Mainz, Germany

* phone +420-54949-4106, fax +420-54949-2840, lammel@recetox.muni.cz

Abstract

Polycyclic aromatic hydrocarbons concentration in air of the central and eastern Mediterranean in summer 2010 was 1.45 (0.30-3.25) ng m^{-3} (sum of 25 PAHs), with 8 (1-17) % in the particulate phase, almost exclusively associated with particles <0.25 μm. The total deposition flux of particulate PAHs was 0.3-0.5 μg m^{-2} $year^{-1}$. The diffusive air-sea exchange fluxes of fluoranthene and pyrene were mostly found net-depositional or close to phase equilibrium, while retene was net-volatilisational in a large sea region. Regional fire activity records in combination with box model simulations suggest that seasonal depositional input of retene from biomass burning into the surface waters during summer is followed by an annual reversal of air-sea exchange, while inter-annual variability is dominated by the variability of the fire season. One third of primary retene sources to the sea region in the

period 2005-2010 returned to the atmosphere as secondary emissions from surface seawaters. It is concluded that future negative emission trends or interannual variability of regional sources may trigger the sea to become a secondary PAH source through reversal of diffusive air-sea exchange.

Capsule: Polycyclic aromatic hydrocarbons phase distributions in marine aerosols, direction of air-sea exchange and open fires as a possible source characterised in the Mediterranean

Keywords: polycyclic aromatic hydrocarbons, long-range transport, air-sea exchange, open fires

1. Introduction

The marine atmospheric environment is a receptor for polycyclic aromatic hydrocarbons (PAHs) which are advected from combustion sources on land (power plants, biomass burning, road transport, domestic heating). Marine sources may be significant near transport routes (ship exhaust). Long-range transport from urban and industrial sources on land are the predominant sources of PAHs in the Mediterranean (Masclet et al., 1988; Tsapakis et. al, 2003 and 2006; Tsapakis and Stephanou, 2005a). A number of PAHs are semivolatile (vapour pressures at 298 K in the range 10^{-6}-10^{-2} Pa) and, hence partition between the gas and particulate phases of the atmospheric aerosol, influenced by temperature, particulate phase chemical composition and particle size (Keyte et al., 2013). Upon deposition to surface water PAHs partition between the aqueous and particulate (colloidal and sinking) phases and may bioaccumulate in marine food chains (Lipiatou and Saliot, 1991; Dachs et al., 1997; Tsapakis

et. al, 2003; Berrojalbiz et al., 2011). They were also found enriched in the sea-surface microlayer relative to subsurface water (Lim et al., 2007; Guitart et al., 2010). Semivolatile PAHs may be subject to re-volatilisation from the sea surface (reversal of air-sea exchange), similar to chlorinated semivolatile organics (Bidleman and McConnell, 1995), in case high concentrations in surface water would build up. This had been predicted by multicompartmental modelling for 2-4 ring PAHs for polluted coastal waters and also the open ocean (Greenfield and Davis, 2005; Lammel et al., 2009a) and was indeed observed in coastal waters off the northeastern United States (Lohmann et al., 2011). Field studies in the open sea found net-deposition to prevail whenever determined (e.g. Tsapakis et al., 2006; Balasubramanian and He, 2010; Guitart et al., 2010; Castro-Jiménez et al., 2012; Mai, 2012). However, some 3-4 ring parent PAHs, among them fluorene (FLN), fluoranthene (FLT) and pyrene (PYR), were reported to be close to phase equilibrium in the Mediterranean, Black and North seas (Castro-Jiménez et al., 2012; Mai, 2012), and net volatilisation of FLT and PYR was observed in the open southeastern Mediterranean Sea in spring 2007 (Castro-Jiménez et al., 2012).

The aim of this study was to add insights on the cycling of PAHs in the Mediterranean in summer, with a focus on sources and phase partitioning in the aerosol.

2. Methods

2.1 Sampling

Gas and particulate phase air samples were taken during the RV Urania cruise, 27 August – 12 September 2010 (see Supplementary Material (SM), Fig. S1). The high volume sampler (Digitel) was equipped with one glass fibre filter (GFF, Whatman) and one polyurethane

70 foam (PUF) plug (Gumotex Břeclav, density 0.030 g cm^{-3}, 50 mm diameter, cleaned by
71 extraction in acetone and dichloromethane, 8 h each, placed in a glass cartridge) in series.
72 Particle size was classified in the particulate phase using high-volume filter sampling (F = 68
73 m^3 h^{-1}, model HVS110, Baghirra, Prague) and low-volume impactor sampling (F = 0.54 m^3 h^{-1}
74 , Sioutas 5-stage cascade, PM_{10} inlet, cutoffs 2.5, 1.0. 0.5, 0.25 µm of aerodynamic particle
75 size and back-up filter, impaction on quartz fibre filters (QFF), SKC Inc., Eighty Four, USA,
76 sampler Baghirra PM_{10-35}). In total 15 high-volume filter samples, exposed 8-36 h (230-1060
77 m^3 of air), and 3 low-volume impactor samples, exposed 5 d, were collected. Water sampling
78 was performed using the stainless steel ROSETTE active sampling device equipped with 24
79 Niskin bottles (volume of 10 l) deployed in water at 1.5 m depth for surface water sampling.
80
81 PAH sampling on GFF and in PUF can be subject to losses related to oxidation of sorbed
82 PAH by ozone (Tsapakis and Stephanou, 2003). This artifact is species-specific and the more
83 pronounced the higher the ozone concentration and the longer the sampling time. Among the
84 PAHs addressed benzo(a)pyrene and pyrene have been identified as particularly vulnerable to
85 oxidation. Based on such sampling artefact quantification studies (Tsapakis and Stephanou,
86 2003; Galarneau et al., 2006) and ozone levels (Table 1a) and sampling times (Table S1) we
87 expect that total PAHs are underestimated by up to 50% in the gas-phase and by up to 25% in
88 the particulate phase.
89 With the aim to characterize the potential influences of ship-bourne emissions on the
90 samples, passive air samplers with PUF disks (150 mm diameter, 15 mm thick, deployed in
91 protective chambers consisting of two stainless steel bowls; Klánová et al., 2008) were

exposed at 5 different locations on board during 16 days. The PAH levels of these samples indicated that ship-based contamination was negligible.

2.2 PAHs analyses and quality assurance

For PAH analysis all samples were extracted with dichloromethane in an automatic extractor (Büchi B-811). Surrogate recovery standards (D8-naphthalene, D10-phenanthrene, D12-perylene) were spiked on each PUF and GFF prior to extraction. The volume was reduced after extraction under a gentle nitrogen stream at ambient temperature, and fractionation achieved on a silica gel column.

The extract was fractionated on a silica column (5 g of silica 0.063 – 0.200 mm, activated 12 h at 150°C). The first fraction (10 mL n-hexane) containing aliphatic hydrocarbons was discarded. The second fraction (20 mL dichloromethane) containing PAHs was collected and then reduced by stream of nitrogen in a TurboVap II (Caliper LifeSciences, USA) concentrator unit and transferred into an insert in a vial. Terphenyl was used as syringe standard, final volume was 200 µL. Gas-chromatography / mass spectrometric analysis was performed on a 6890N GC equipped with a 60m x 0.25mm x 0.25µm DB5-MS column (Agilent J&W, USA) coupled to 5973N MS (Agilent, USA). The MS was operated in electron impact positive ion mode with selected ion recording (SIR).The targeted compounds are the 16 EPA priority PAHs (i.e., naphthalene (NAP), acenaphthylene (ACY), acenaphthene (ACE), fluorene (FLN), phenanthrene (PHE), anthracene (ANT), fluoranthene (FLT), pyrene (PYR), benzo(a)anthracene (BAA), chrysene (CHR), benzo(b)fluoranthene (BBF), benzo(k)fluoranthene (BKF), benzo(a)pyrene (BAP), indeno(123cd)pyrene (IPY), dibenzo(ah)anthracene (DBA), benzo(ghi)perylene (BPE)), 10 more parent PAHs (i.e.,

benzo(ghi)fluoranthene (BGF), cyclopenta(cd)pyrene (CPP), triphenylene (TPH), benzo(j)fluoranthene (BJF), benzo(k)fluoranthene (BKF), benzo(e)pyrene (BEP), perylene (PER), dibenz(ac)anthracene (DCA), anthranthrene (ATT), and coronene (COR)), and one alkylated PAH, retene (RET). The injection volume was 1 µL. Terphenyl was used as internal standard.

Field blank values, b, were gained from GFFs and PUFs manipulated in the field, as far as possible identical to the samples, except without switching the high-volume sampler on. No QFF field blank was taken for impactor sampling. As no PAHs were detected in the stages corresponding to 2.5-10 µm (all PAHs < limit of detection in all such samples), instead the mean of values of the QFF substrates of the 2 uppermost impactor stages (in total 6) was taken. The respective b value was subtracted from sample values. The limit of quantification needs to take the accuracy of the blank level into account. In lack of a measure for the variation of the field blank, the relative standard deviation (SD) of field blanks from earlier field campaigns, (σ_c/b_c), on a high-mountain site (high-volume sampling summer 2007, n = 5; Lammel et al., 2009b) and in the Mediterranean (impactor sampling summer 2008, n = 6; Lammel et al., 2010a) was used ($\sigma = (\sigma_c/b_c) \times b$). Identical samplers, sampling and analysis protocols for all analytes had been applied. Values below the sum of the field blank value (from this campaign) and 3 relative SDs of the field blank values (from the previous campaigns) were considered <LOQ (limit of quantification, LOQ = b + 3σ). NAP and ACY were excluded from the data set, because of the lack of blank values. The field blank values of most other analytes were below instrument LOQ in high-volume PUF and GFF samples. However, higher field LOQs, up to (6-25) pg m^{-3} (according to sampled volume of air) resulted for ANT, PYR and RET, and up to (45-180) pg m^{-3} for ACE, FLN, PHE and FLT in

PUF. Field LOQs of PAHs in impactor QFF samples were below instrumental LOQ for most substances, but in the range (8-15) pg m^{-3} for ACE, ANT, and FLT, ≈55 pg m^{-3} for FLN, and 120-140 pg m^{-3} for NAP and PHE.

The instrument limit of quantification (LOQ), which is based on the lowest concentration of calibration standards used, was 0.5 ng, corresponding to 0.5-2.5 pg m^{-3} for high-volume samples, ≈8 pg m^{-3} for impactor samples, 6-10 pg m^{-3} for semivolatile PAHs determined in passive air samples and up to 200 pg m^{-3} for non volatile PAHs in passive air samples.

Water samples (2-2.5 L) were extracted immediately after their collection using solid phase extraction on C_{18} Empore discs using a vacuum manifold device. Disks were stored closed in glass vials in a freezer and transported to the processing laboratory, PAHs were eluted from disks using 40 mL of dichloromethane. The above listed PAHs were analysed on GC/MS (Agilent GC 6890N coupled to an Agilent single quadrupole MS 5973N operating in electron impact ionisation mode). LOQ was 0.1 ng L^{-1}.

Other trace constituents and meteorological parameters

Ozone was measured with an absorption method (Teledyne–API model 400A UV) on the top deck (10 m above sea surface). Meteorological parameters (air temperature, humidity, wind direction and velocity) and oceanographic parameters were determined aboard.

2.3 Models of gas-particle partitioning

The data set (15 high-volume samples of separate gas and particulate phase concentrations) is used to test gas-particle partitioning models for semivolatile organics in terms of the organics' mass size distribution and size dependent particulate matter (PM) composition. The

models assume different processes to determine gas-particle partitioning, i.e. an adsorption model (Junge-Pankow; Pankow, 1987), and two absorption models (i.e. K_{OA} models; Finizio et al., 1997; Harner and Bidleman, 1998). Absorption is into particulate organic matter (OM). Adsorption to soot is a significant gas---particle partitioning processes for PAHs, but no soot data or PM chemical composition data are available. We, therefore, refrain from testing dual adsorption and absorption models (e.g. Lohmann and Lammel, 2004). Particulate mass fraction, θ, and partitioning coefficient, K_p, are defined by the concentrations in the 2 phases:

$$\theta = c_p / (c_p + c_g)$$

$$K_p = c_p / (c_g \times c_{TSP}) = \theta / [(1 - \theta) \times c_{TSP}]$$

With PAH particulate and gas-phase concentrations c_p and c_g in units of ng m^{-3}, c_p representing the whole particle size spectrum, concentration of total suspended matter, c_{TSP}. Different models describe different processes to quantify differences in ad- and absorption between compounds. The Junge-Pankow model uses the vapour pressure of the sub-cooled liquid p_L^0, $\theta = c_J S/(p_L^0+c_J S)$, (data taken from Lei et al., 2002), c_J should be approximately 171 Pa cm for PAHs (Pankow, 1987). The aerosol particle surface concentration, S, was not measured and a typical value for maritime aerosols is adopted instead (4.32×10^{-7} cm^{-1}; Jaenicke, 1988). Harner and Bidleman, 1998, use the log K_{OA} and f_{OM}: $\log K_p = \log K_{OA} + \log f_{OM} - 11.91$; and Finizio et al., 1997, uses only the K_{OA} as predictor (data taken from Ma et al., 2010): $\log K_p = 0.79 \times \log K_{OA} - 10.01$. The range of the fraction of OM used here is based on Putaud et al., 2004 (16% lower limit) and Spindler et al., 2012 (45% upper limit).

184

185 **2.4 Air-sea diffusive mass exchange calculations**

186 State of phase equilibrium is addressed by fugacity calculation, based on the Whitman two-
187 film model (Liss and Slater, 1974; Bidleman and McConnell, 1995**)**. The fugacity ratio (FR)
188 is calculated as:

189

190 $FR = f_a/f_w = C_a R T_a / (C_w H_{Tw,salt})$

191

192 with fugacities from air and water, f_a and f_w, gas-phase concentration C_a (ng m^3), dissolved
193 aqueous concentration C_w (ng m^3), universal gas constant R (Pa m^3 mol^{-1} K^{-1}), water
194 temperature and salinity corrected Henry's law constant $H_{Tw,salt}$ (Pa m^3 mol^{-1}), and air
195 temperature T_a (K). C_w is derived from the bulk seawater concentration, C_{bulk}:

196

197 $C_w = C_{bulk} /(1 + K_{POC} C_{POC} + K_{DOC} C_{DOC})$

198

199 with particulate and dissolved organic carbon concentrations, C_{POC} and C_{DOC}, from Pujo-Pay
200 et al., 2011, K_{POC} and K_{DOC} from Karickhoff, 1981, Lüers and ten Hulscher 1996, Rowe et al,
201 2009, and Ma et al, 2010. Values 0.3< FR <3.0 are conservatively considered to not safely
202 differ from phase equilibrium, as propagating from the uncertainty of the Henry's law
203 constant, $H_{Tw,salt}$, and measured concentrations (e.g., Bruhn et al., 2003; Castro-Jiménez et al.,
204 2012; Zhong et al., 2012). This conservative uncertainty margin is also adopted here, while
205 FR >3.0 indicates net deposition and FR <0.3 net volatilisation. The diffusive air–seawater

gas exchange flux (F_{aw}, ng m^{-2} day^{-1}) is calculated according to the Whitman two-film model (Bidleman and McConnell, 1995; Schwarzenbach et al., 2003):

$$F_{aw} = k_{ol} (C_w - C_a RT_a / H_{Tw,salt})$$

with air-water gas exchange mass transfer coefficient k_{ol} (m h^{-1}), accounting for resistances to mass transfer in both water (k_w, m h^{-1}) and air (k_a, m h^{-1}), defined as

$$1/k_{ol} = 1/k_w + RT_a/(k_a H_{Tw,salt})$$

with $k_a = (0.2U_{10} + 0.3)*(D_{i,air}/D_{H2O,air})^{0.61} \times 36$, $k_w = (0.45U_{10}^{1.64}) \times (Sc_i/Sc_{CO2})^{-0.5} \times 0.01$. U_{10} is the wind speed at 10 meter height above sea level (m s^{-1}), $D_{i,air}$ and $D_{H2O,air}$ are the temperature dependent diffusivities of substance *i* and H_2O in air, and Sc_i and Sc_{CO2} are the Schmidt numbers for substance *i* and CO_2 (see Bidleman and McConnell, 1995; Zhong et al. 2012; and references therein). U_{10}, T_a, T_w and air pressure are taken from the ship based measurements.

2.5 Non-steady state 2-box model

The air–sea mass exchange flux of RET is simulated by a non-steady state zero-dimensional model of intercompartmental mass exchange (Lammel, 2004). RET is selected, because of the prevalence of one dominating source. This 2-box model predicts concentrations by integration of two coupled ordinary differential equations that solve the mass balances for the two compartments, namely the atmospheric marine boundary layer (MBL) and seawater

229 surface mixed layer. Processes considered in air are dry (particle) deposition, removal from
230 air by reaction with the hydroxyl radical, and air-sea mass exchange flux (dry gaseous
231 deposition), while in seawater export (settling) velocity, deposition flux from air, air-sea
232 mass exchange flux (volatilisation), and degradation (as 1^{st} order process) are considered. All
233 input parameters are listed in the SM, Table S2.
234 Atmospheric depositions related to emissions from open fires are assumed to provide the
235 only source for seawater RET. These are available as daily time series for the East
236 Mediterranean domain (28-45°N, 8-30°E) through the fire-related $PM_{2.5}$ emissions as
237 provided by the Global Fire Assimilation System (GFASv1.0; Kaiser et al., 2012) in
238 combination with an emission factor (207 mg RET in $PM_{2.5}$ (kg fuel burnt)$^{-1}$; Schmidl et al.,
239 2008). The fire emissions are averaged over the domain and assumed to disperse within the
240 MBL only. This is justified due to the assumed underestimation of the fire related emissions
241 and ignorance of other (emission) sources. The 2-box model is run for the years 2005-2010,
242 for the east Mediterranean domain (28-45°N, 8-30°E) with a 1 h time resolution. Air–sea
243 mass exchange fluxes, F_{em}, in the range (0.30 ± 1.46) ng m^{-2} h^{-1} (positive defined upward) are
244 simulated (using the initially estimated parameter set, Table S2). GFAS uses global satellite
245 observations of fire radiative power to estimate daily dry matter combustion rates and fire
246 emission fluxes. The GFAS system partly corrects for observational gaps (e.g. due to cloud
247 cover) and detects fires in all biomes, except for very small fires (lower detection limit of
248 around 100-1000 m^2 effective fire area).
249
250 **2.6 Analysis of long-range advection of air**

Distributions of potential sources can be identified by inverse modelling using meteorological input data (Stohl et al., 2003; Eckhardt et al., 2007). So-called retroplumes are generated using operational weather prediction model data and a Lagrangian particle dispersion model, FLEXPART (Stohl et al., 1998, 2005). Hereby, 50000 virtual particles per hour were 'released' and followed backwards in time for 5 days. The model output is a 3-D distribution of residence time.

3. Results and discussion

3.1 PAH concentrations in air and seawater

The mean total (i.e., sum of gaseous and particulate) Σ25 PAHs concentration is 1.45 ng m^{-3} (time-weighted; 1.54 with values <LOQ replaced by LOQ/2, see Table 1a), and ranged from 0.30-3.25 ng m^{-3}. The spatial variability of PAH levels in the Mediterranean is large, determined by long-range advection (Tsapakis and Stephanou, 2005a; Tsapakis et al., 2006). The levels found in this study in the southeastern Mediterranean are for most substances lower than found earlier (Table 2). In the Ionian Sea and Sicily region (ISS) some PAHs are found somewhat higher than previously measured i.e., FLT and PYR (in the gas-phase) and BAP and PER (in the particulate phase). Due to a sampling artefact BAP and other particulate phase PAHs could be underestimated by up to 25% (aforementioned, section 2.1). The seasonality of emissions and the variability of advection or advection in combination with different cruise routes being influenced differently by coastal or ship emission plumes can have a large influence and may explain these differences. On the other hand, the duration of temporal averaging atmospheric concentrations was similar across the various studies. Diagnostic ratios (BAA/(BAA+CHR), FLT/(FLT+PYR); Dvorská et al., 2011) in some of the

274 samples (No. 2, 4, 7, 8, and 15) reflect the influence of traffic and industrial sources. We
275 investigated the potential source distribution of individual samples collected along the cruise
276 (section 2.6) and found that indeed maxima of PAH concentrations corresponded with air
277 masses having resided over large urban areas, and, vice versa, low concentrations
278 corresponded with air masses without apparent passage of such areas (illustrated in Fig. S4).
279 This finding is supported by the ozone data i.e., 53 (47-65) ppbv during influence from urban
280 areas but 37 (33-62) ppbv otherwise.
281 It had been pointed out that the source distribution around the Mediterranean may cause a
282 west-east gradient, leading to higher concentrations found in the ISS than in the southeastern
283 Mediterranean (SEM; Berrojalbiz et al., 2011). This gradient is somewhat reflected in our
284 results, as levels in the ISS exceeded levels in the SEM (Table 2).
285 Most PAH concentrations in surface seawater were <LOQ, while FLT, PYR and RET were
286 quantified in at least part of the samples (Table 1b). These observed seawater contamination
287 levels are comparable to levels found in the region 2 and 1 decades ago (Lipiatou et al.,
288 1997; Tsapakis et al., 2003). The concentrations near Crete (samples No. 7 and 8a) are very
289 similar to those found in fall 2001 and winter-spring 2002 (Tsapakis et al., 2006; FLT = 0.15
290 (0.11-0.21) ng L^{-1} , PYR = 0.12 (0.07-0.17) ng L^{-1}).
291
292 Table 1. Concentrations of PAHs found in (a.) air (total, i.e. sum of gas and particulate
293 phases, ng m^{-3}) and (b.) seawater (total, i.e. sum of dissolved and particulate, ng L^{-1}) as time-
294 weighted mean (min-max). n_{LOQ} = number of samples > LOQ (out of 15 air and 23 seawater
295 samples). PAHs with concentrations <LOQ in all samples not listed. For calculation of mean
296 values <LOQ were replaced by LOQ/2. Ozone levels are given, too (ppbv).

297 a)

	n_{LOQ}	mean (min-max)
ACE	4	0.025 (<0.020–0.089)
FLN	10	0.137 (<0.030–0.396)
PHE	15	0.581 (0.144–1.41)
ANT	13	0.043 (0.008–0.22)
RET	14	0.016 (0.006–0.030)
FLT	15	0.262 (0.053–0.795)
PYR	15	0.203 (0.044–0.564)
BAA	15	0.01 (0.0014–0.031)
CHR	15	0.04 (0.012–0.092)
TPH	15	0.018 (0.007–0.032)
BBN	11	0.018 (0.001–<0.085)
BBF	15	0.021 (0.004–0.102)
BKF	14	0.012 (0.002–<0.085)
BAP	12	0.015 (0.001–<0.085)
BGF	15	0.021 (0.005–0.067)
CPP	7	0.012 (0.001–<0.085)
BJF	15	0.016 (0.002–0.079)
BEP	14	0.019 (0.004–0.088)
PER	7	0.012 (0.001–0.1)
IPY	7	0.022 (0.008–0.094)

BPE	6	0.02 (0.009–0.085)
COR	5	0.016 (0.002–0.1)
Σ25 PAHs		1.539 (0.44–4.694)
Ozone		42 (33 – 65)

298

299 b)

	n_{LOQ}	mean (min-max)
PHE	1	1.1
RET	12	0.1 (<0.1–0.5)
FLT	10	0.1 (<0.1–0.3)
PYR	7	0.2 (<0.2–0.9)

300

301 Table 2 Gaseous (a) and particulate (b) concentrations in air (time-weighted mean (min-
302 max), ng m^{-3}) of selected PAHs compared to other studies in the Ionian Sea and Sicily region
303 (ISS) and in the southeastern Mediterranean (SEM). For calculation of means values <LOQ
304 were replaced by LOQ/2. RV = research vessel cruise.

305 a)

	ISS		SEM			
	RV August-September 2010	RV June 2006, May 2007	RV August-September 2010	RV June 2006, May 2007	Finokalia September-October 2001, February, March and July 2002 (1)	Finokalia November 2000-February 2002(2)

	this study	Castro-Jiménez et al., 2012	this study	Castro-Jiménez et al., 2012	Tsapakis et al. 2006	Tsapakis & Stephanou 2005a
FLN	0.16 (<0.027–0.34)	2.25 (1.27–5.65)	0.071 (<0.050–0.40)	0.69 (0.36–1.23)	1.05 (0.15–1.67)	1.8 (0.2–5.7)
PHE	0.52 (0.14–1.11)	7.00 (3.52–15.45)	0.35 (0.14–1.41)	3.94 (2.50–6.35)	4.78 (1.75–7.78)	7.3 (1.5–27.7)
ANT	0.040 (<0.021–0.10)	0.37 (0.18–0.55)	0.039 (<0.013–0.22)	0.20 (0.16–0.30)	0.61 (0.12–1.31)	0.9 (0.1–4.5)
FLT	0.14 (0.053–0.31)	0.05 (0.02–0.07)	0.10 (0.061–0.37)	0.007 (0.003–0.011)	0.82 (0.12–1.69)	1.8 (0.07–6.0)
PYR	0.14 (0.058–0.56)	0.04 (0.02–0.06)	0.12 (0.044–0.29)	0.006 (0.003–0.009)	0.65 (0.14–0.97)	0.9 (0.1–2.8)
CHR	0.012 (0.0071–0.021)	0.09 (0.03–0.23)	0.014 (0.012–0.037)	0.03 (0.02–0.05)	0.18 (0.06–0.33)	0.2 (<0.001–0.6)
Sum of 6 PAHs	1.0	9.8	0.7	4.9	8.1	12.9

b)

	ISS		SEM		
	RV August-	RV June 2006, May 2007	RV August-September	RV June 2006, May	Finokalia November 2000-

	September 2010		2010	2007	February 2002
	this study	Castro-Jiménez et al., 2012	this study	Castro-Jiménez et al., 2012	Tsapakis & Stephanou 2005a
FLN	<0.92 (<0.60–<1.1)	0.001 (0.0009–0.002)	<0.66 (<0.33–<1.4)	0.0013 (0.0011–0.0016)	0.02 (<0.001–0.01)
PHE	<1.9 (<1.2–<2.3)	0.06 (0.01–0.12)	<1.6 (<0.66–<2.7)	0.04 (0.01–0.13)	0.05 (0.004–0.2)
ANT	<0.21 (<0.14–<0.26)	0.007 (0.0009–0.012)	<0.16 (<0.07–<0.32)	0.009 (0.0007–0.023)	0.004 (<0.001–0.02)
FLT	<0.85 (<0.56–<1.0)	0.099 (0.01–0.19)	<0.62 (<0.30–<1.3)	0.049 (0.01–0.12)	0.1 (0.04–0.2)
PYR	<0.11 (<0.070–<0.13)	0.109 (0.016–0.216)	<0.08 (<0.044–<0.16)	0.057 (0.012–0.142)	0.04 (0.01–0.01)
BAA	0.0054 (<0.0018–0.025)	0.013 (0.006–0.023)	0.0026 (<0.0006–0.0080)	0.018 (0.004–0.046)	0.03 (0.003–0.1)
CHR	0.018 (0.0030–0.076)	0.04 (0.01–0.08)	0.0079 (0.0033–0.020)	0.043 (0.012–0.101)	0.1 (0.02–0.3)
BBF	0.023	0.029 (0.012–	0.011	0.033 (0.010–	0.04 (<0.001–0.2)

	(<0.0018–0.010)	0.045)	(0.0042–0.033)	0.060)	
BKF	0.012 (<0.0018–0.057)	0.015 (0.005–0.027)	0.0047 (0.0018–0.015)	0.089 (0.005–0.333)	0.04 (<0.001–0.2)
BAP	0.013 (<0.0009–0.072)	0.009 (0.04–0.016)	0.0046 (<0.0011–0.0098)	0.034 (0.005–0.081)	0.02 (0.01–0.05)
BJF	0.018 (<0.0018–0.079)	0.015 (0.014–0.016)	0.0072 (0.0023–0.031)	0.010 (0.008–0.011)	-
BEP	0.019 (<0.0018–0.088)	0.03 (0.02–0.05)	0.0082 (0.0035–0.025)	0.046 (0.017–0.093)	0.04 (0.01–0.1)
PER	0.0023 (<0.00096–0.011)	0.002 (0.0005–0.004)	0.00075 (<0.0006–0.0021)	0.026 (0.0001–0.068)	0.004 (<0.001–0.01)
IPY	0.015 (<0.00096–0.094)	0.018 (0.006–0.032)	0.0016 (<0.00052–0.019)	0.009 (0.002–0.013)	0.03 (0.009–0.2)
BPE	<0.0014 (<0.00096–0.0018)	0.026 (0.017–0.042)	0.0041 (<0.00052–0.020)	0.081 (0.012–0.210)	0.03 (0.010–0.09)
Sum of 15 PAHs	0.09	1.06	0.05	0.54	0.54

308 (1) months Sep and Oct 2001, Feb, Apr and May 2002. No particulate data reported.

309 (2) 24h per month between Feb 2000 and Feb 2002

310

311 **3.2 Gas-particle partitioning**

312 Only a small mass fraction of the total, $\theta = 0.08$, is found in the particulate phase, confirming
313 earlier findings from remote sites in the region (Tsapakis and Stephanou, 2005a; Tsapakis et
314 al., 2006; Table 3c). The particulate mass fraction, θ, of four semivolatile PAHs varied
315 considerably along the cruise track (see SM Fig. S2). θ is thought to be strongly influenced
316 by temperature and doubling per 13 K cooling was found in a Mediterranean environment
317 (Lammel et al., 2010b) apart from PM composition. We refrain from an exploration of the
318 vapour pressure (p_L^0) dependence of θ (or K_p): A low time resolution implies lack of
319 representativeness of the temperature measurement for the phase change (Pankow and
320 Bidleman, 1992). Furthermore, non-equilibrium conditions cannot be excluded (but are
321 likely as a consequence of time resolution; Hoff et al., 1998), and supporting physical and
322 chemical aerosol parameters, necessary to relate to, are lacking. For similar temperatures
323 higher θ values had been observed at sites on the region influenced by urban and industrial
324 sources (Mandalakis et al., 2002; Tsapakis and Stephanou, 2005b; Akyüz and Çabuk, 2010),
325 which is probably related to the influence of higher organic and soot PM mass fractions. Gas-
326 particle partitioning models (Table 3) underpredict θ, except the Finizio et al., 1997, model
327 for one substance, TPH. θ predicted by the Junge-Pankow (JP) model comes closest. A
328 number of semivolatile PAHs could not be included in this test of gas-particle partitioning
329 models as concentrations in either the gas-phase (CPP, BBF, BJF), or the particulate phase
330 (FLT, PYR, BBN) did not exceed LOQ or no insufficient input data were available (BBF).

331 The neglect of adsorption to soot, not covered by the gas-particle partitioning models tested,
332 may explain at least part of the underprediction (Lohmann and Lammel, 2004). Due to the
333 lack of organic and elemental carbon data an extended examination is not possible.
334 In size-segregated samples particulate PAH mass was almost exclusively found in the size
335 fraction <0.25 μm aerodynamic diameter (AD) (<LOQ in the other stages, except 0.002 ng
336 m^{-3} CPP in the size fraction corresponding to 0.5-1.0 μm; S2.1, Table S4). Most particulate
337 phase PAHs, 40%, have been found associated with particles <0.5μm out of 5 size ranges in
338 the marine background aerosol of the sea region (coast of Crete, November 1996 – June
339 1997; Kavouras and Stephanou, 2002). At continental sites in central and southern Europe
340 mass median diameters of PAHs were found to be in the accumulation range, mostly 0.5-1.4
341 μm (Schnelle et al., 1995; Kiss et al., 1998; Lammel et al., 2010b and 2010c), but also a
342 second, coarse mode was found (up to 2.4 μm; Chrysikou et al., 2009).
343
344 Table 3. Gas-particle partitioning of selected PAHs (mean ± sd (median)), observed and
345 predicted by the models Junge-Pankow, 1987 (JP), Harner and Bidleman, 1998 (HB), and
346 Finizio et al., 1997 (F), expressed as (a) particulate mass fraction, θ, and (b) log K_p of this
347 study.
348 a)

	Observed	JP	HB	F
BAA	0.51 ± 0.28 (0.47)	0.18 ± 0.07 (0.18)	0.08 – 0.20	0.18
TPH	0.27 ± 0.13 (0.26)	0.24 ± 0.10 (0.24)	0.23 – 0.46	0.37
CHR	0.35 ± 0.15 (0.35)	0.31 ± 0.13 (0.32)	0.09 – 0.21	0.19
BBF	0.88 ± 0.40 (0.94)	0.91 ± 0.40 (0.97)	0.49 – 0.73	0.59

b)

	Observed	JP	HB	F
BAA	-1.28 ± 1.00 (-0.96)	-1.97 ± 1.14 (-1.84)	-2.43 – -1.98	-1.89
TPH	-1.77 ± 1.27 (1.45)	-1.80 ± 1.07 (-1.63)	-1.91 – -1.46	-1.48
CHR	-1.59 ± 1.18 (1.34)	-1.65 ± 1.01 (-1.46)	-2.41 – -1.96	-1.87
BBF	-0.94 ± 0.19 (-0.24)	-0.52 ± 0.66 (-0.74)	-1.41 – -0.96	-1.08

3.3 Fugacity ratio and air-sea exchange flux

Fugacity ratios (Fig. 1a) and vertical fluxes (Fig. 1b) could be quantified for FLT, PYR and RET. The uncertainty window of FR = f_a/f_w = 0.3 - 3.0 is based on the uncertainty of $H_{Tw,salt}$. Values FR >3.0 indicate net deposition, FR <0.3 indicate net volatilisation. For RET both water and air concentrations of sample No. 2 were <LOQ. Transfer coefficients were k_w << k_a.

a.

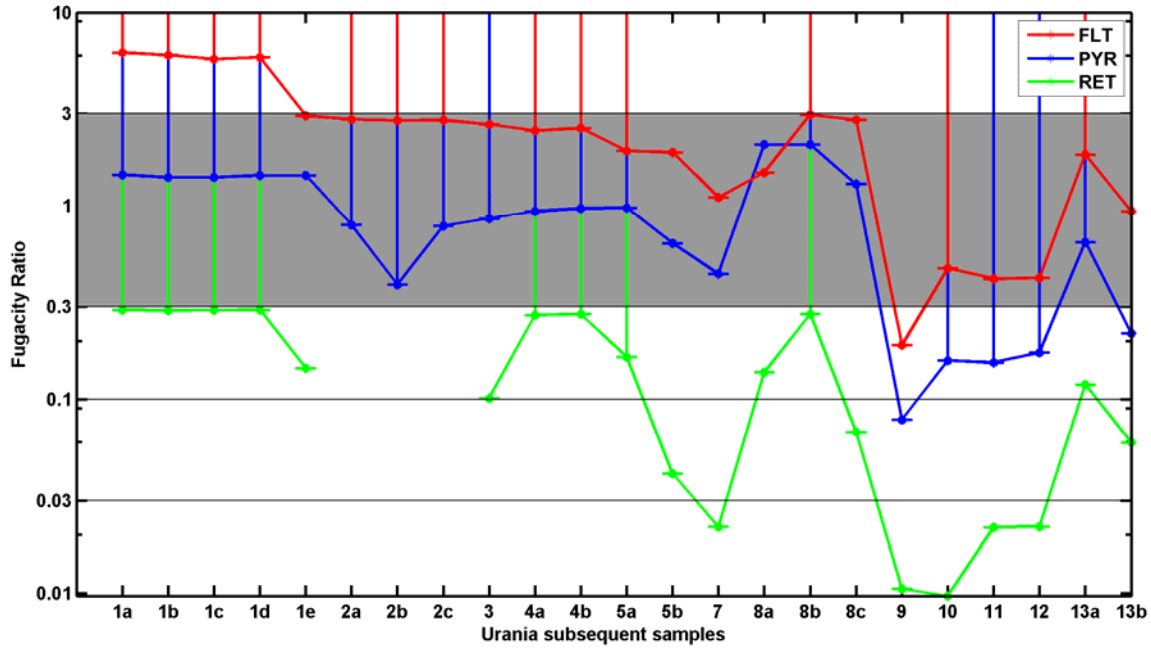

359

360 b.

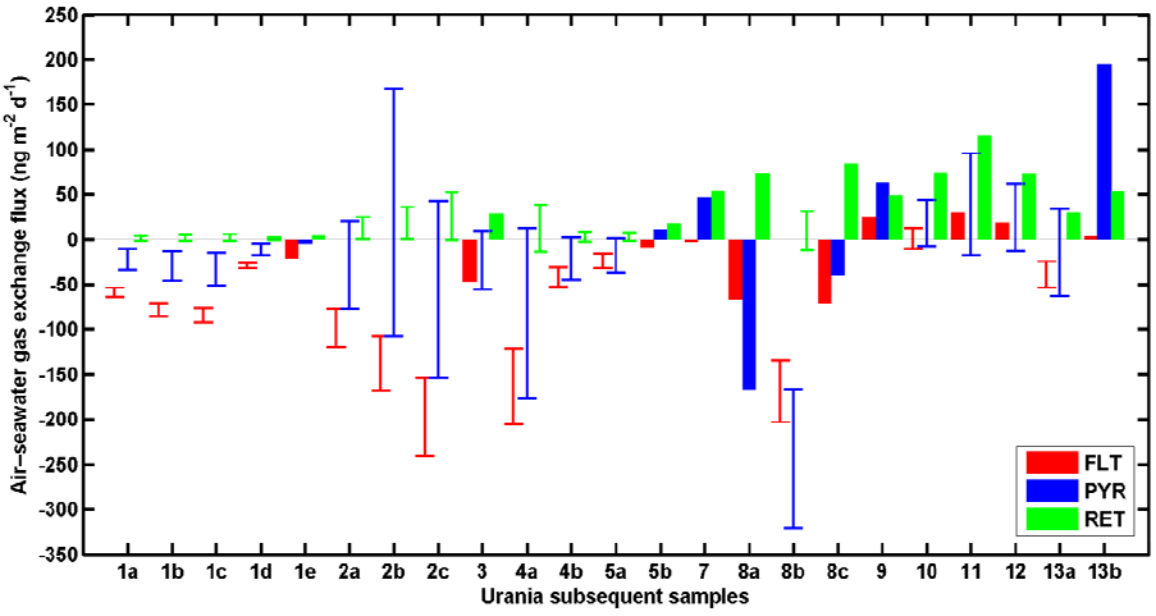

361

362 Fig. 1. Air-sea exchange, (a) fugacity ratios FR = f_a/f_w (volatilisation > 3, deposition < 0.3,

363 grey area insignificant deviation from phase equilibrium) and (b) flux F_{aw} (ng m^{-2} d^{-2};

364 volatilisation > 0, deposition < 0) of FLT, PYR and RET along the cruise of RV Urania. Error

365 bars indicate sea water concentration C_w <LOQ. The x-axis depicts the correspondence of
366 sequential pairs of air samples (1-13) and water samples (a-e).
367
368 FLT and PYR were found to be close to phase equilibrium, with most of the FR values within
369 the uncertainty range, one sample (No. 1) indicating deposition of FLT and one or two (No. 9
370 and 13) indicating volatilisation of FLT and PYR, respectively. In comparison with earlier
371 observations of FLT and PYR air-sea exchange in the SEM in 2001-02 and 2007 (Tsapakis et
372 al., 2006; Castro-Jiménez et al., 2012) and considering spatial and temporal variabilities no
373 trend, in particular no reversal of air-sea exchange is indicated. This comparison is detailed
374 in the SM, S2.2.1. RET, however, is found net-volatilisational throughout most of the cruise
375 (Fig. 1). Among the highest fluxes (> 50 ng m^2 d^{-1}) are some samples with very low FR,
376 <0.03. Fugacity of RET from water is supported by its Henry's law coefficient (11 Pa m^3
377 mol^{-1} at 298 K) which is higher than for CHR (0.53 Pa m^3 mol^{-1}) and FLT (2.0 Pa m^3 mol^{-1}).
378 RET is commonly considered as biomarker for coniferous wood combustion (Ramdahl,
379 1983). A decrease in wildfires could explain the suspected RET volatilisation. Integrated over
380 the domain and the year 2010, fires released 7.2 PJ fire radiative energy, which translates into
381 around 22.2 Gg of $PM_{2.5}$ emitted (Fig. 2). Compared to the $PM_{2.5}$ emissions of the years 2003
382 to 2012, the year 2010 had the lowest emissions, equivalent to 46% of the 2003-2012 mean,
383 and only 18% of the peak emissions of the year 2007 (Fig. 2d). As typical for the East
384 Mediterranean region, the fire season in 2010 started by the end of June and ended by early
385 October. The Urania cruise measurements took place between 27.8. and 12.9., i.e. towards
386 the end of the main burning season (Fig. 2c). During the first half of the Urania cruise,
387 widespread fire activity was observed in the entire domain, with most intense fires occurring

388 in Southern Italy, Sicilia and along the East coast of the Adriatic and the Ionian Sea (notably
389 in Albania and Greece) (Fig. 2a).
390

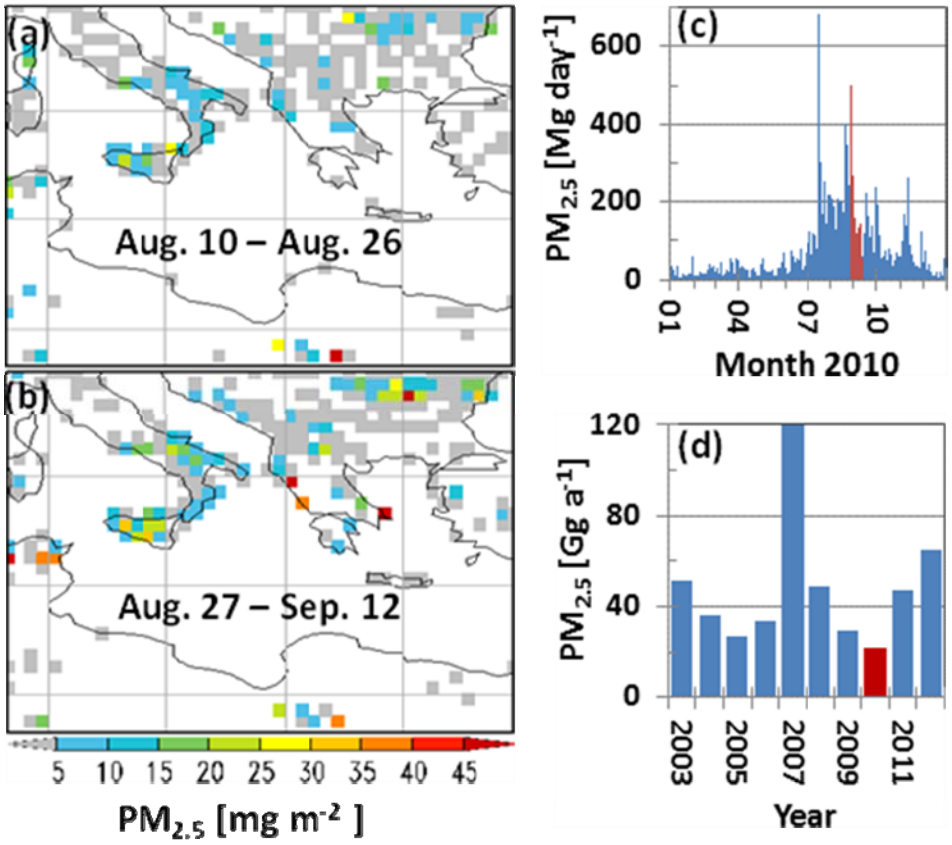

391

392 Fig. 2. Spatial pattern of fire-related $PM_{2.5}$ emissions (Global Fire Assimilation System
393 GFASv1.0; Kaiser et al., 2012) for the East Mediterranean (28-45°N/8-30°E), (a) time
394 integral of August 10-26, (b) time integral of August 27 - September 12, 2010, given as sum
395 over each period in mg m^{-2}. Areas with no observed fire activity are displayed in white.
396 Temporal pattern of domain-integrated (c) daily total $PM_{2.5}$ emissions over 2010 (c) and
397 yearly total $PM_{2.5}$ emissions over 2003 to 2012. Labelled in red is (c) the the period of the
398 Urania cruise (27 August – 11 September 2010) (d) and the year 2010.
399

400 The hypothesis that seasonal depositional input of RET into the surface waters during the fire
401 season (summer) triggers reversal of diffusive air-sea exchange, at least in the year 2010, are
402 tested by box model (sections 2.5 and S1.3) runs. Two scenarios are considered, an 'Initially
403 Estimated Parameter Set' (IEPS) representing mean values for environmental parameters, and
404 an 'Upper Estimate Parameter Set' (UEPS) which represents realistic environmental
405 conditions favouring seawater pollution (SM, Table S3). Simulated diffusive air-sea
406 exchange flux, F_{aw}, during 2005-2010 initialised by the UEPS is shown in Fig. 3a and by the
407 IEPS in the SM, Fig. S3, and during the observations (cruise of RV Urania, 27.8.-9.9.2010)
408 initialised by the UEPS in Fig. 3b.
409 The model confirms the hypothesis that seasonal depositional input of RET into the surface
410 waters during the fire season (July-September, typically in the range $F_{aw} = 10^{-2}$-10^{1} ng m^{-2} d^{-1}
411 under IEPS) is followed by a period of prevailing flux reversal, typically $F_{aw} = 10^{-2}$-10^{0} ng
412 m^{-2} d^{-1}, which in the years 2008-10 started in October and lasted until the onset of the fire
413 season, but eventually started later in the years 2005-07 (at least under IEPS). The
414 volatilisation flux is predicted smaller in magnitude than the net-deposition flux during the
415 fire season, but correspondingly, i.e. higher after intense fire seasons. The high RET
416 volatilisation flux, indicated by measured C_a and C_w, seems to be dominated by biomass
417 burning in the region in the previous fire season. F_{aw} is predicted highly fluctuating, also
418 during the observational period (Fig. 3b). Even under UEPS the model is underpredicting F_{aw}
419 (Fig. 3b). The sensitivity to input uncertainties (SM S1.2) may explain part of the
420 underestimate, but not up to one order of magnitude. Neglected RET sources to seawater,
421 such as riverine input may explain part of the discrepancy.
422

423 a.

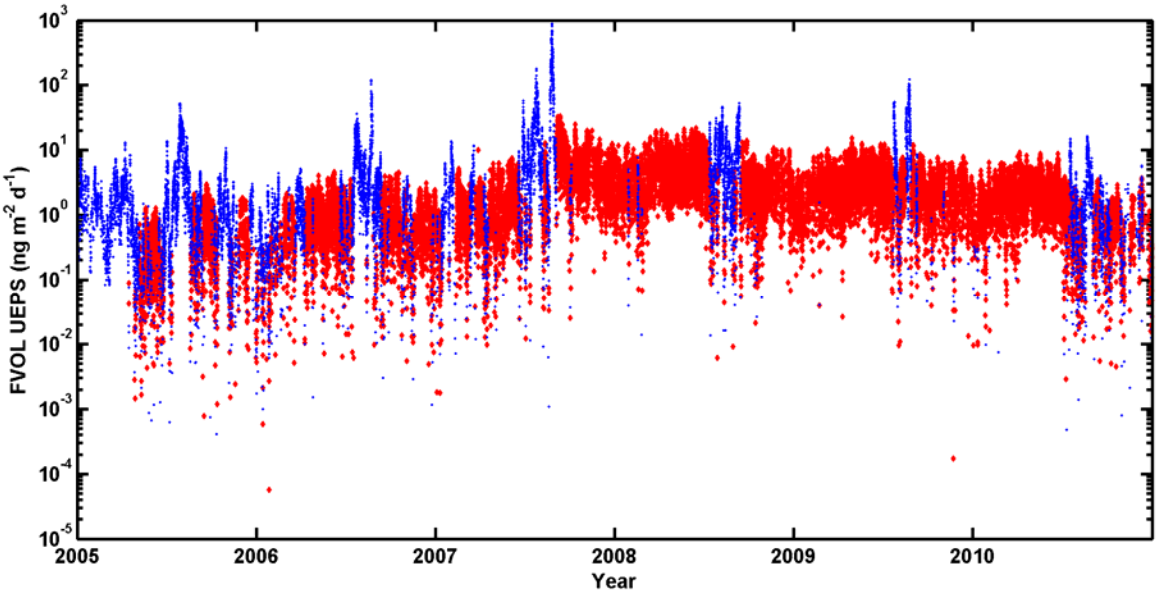

424

425

426 b.

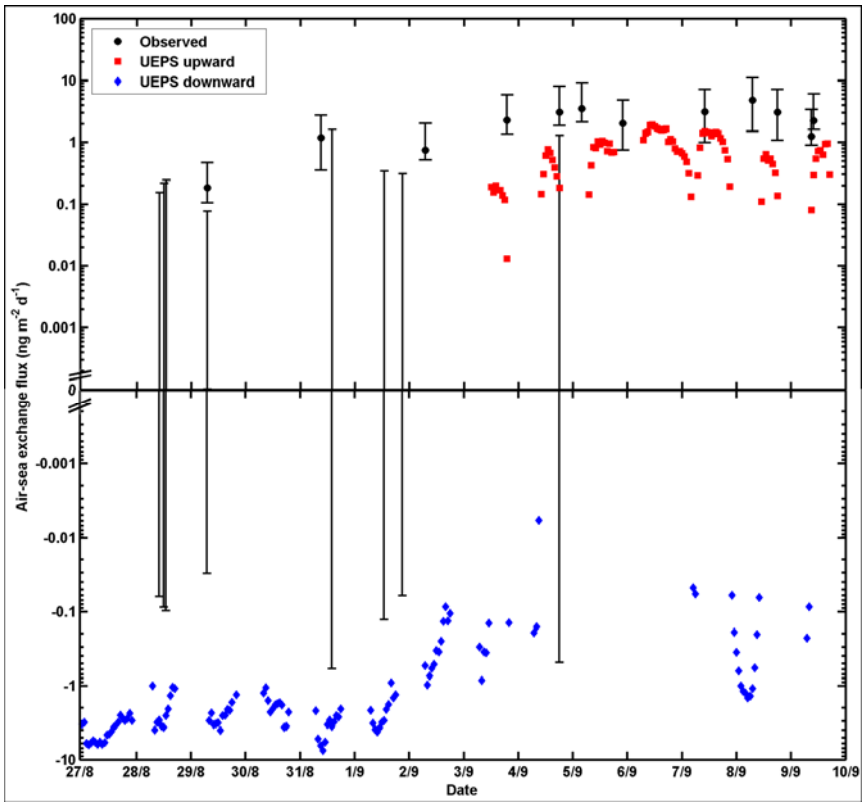

427

Fig. 3. Diffusive air-sea exchange flux, F_{aw}, of RET (ng m^{-2} d^{-1}; downward in blue and upward in red) using the upper estimate parameter set (UEPS) for the Eastern Mediterranean (28-45°N/8-30°E) (a.) model predicted for 1.1.2005-31.12.2010 and (b.) model predicted and observed (black) for 27.8.-9.9.2010. Hourly mean data filtered against off-shore winds (see text). Error bars including both signs of F_{aw} reflect C_w <LOQ.

4. Conclusions

PAH pollution of the atmospheric Mediterranean environment was below previous observations at the beginning of the decade (2001-02; Tsapakis and Stephanou, 2005a; Tsapakis et al., 2006), also considering possible losses during sampling. This might reflect emission reductions. The particulate phase PAHs were concentrated in the size fraction < 0.25 μm AD. The residence time in the troposphere is longest for particles around 0.2 μm of size, with ≈0.01 cm s^{-1} being a characteristic corresponding dry deposition velocity (Franklin et al., 2000), which translates into a residence time of ≈120 days in the MBL (depth of 1000 m; see Table S3) and deposition flux $F_{dep} = c \times v$ = 0.03-0.06 μg m^{-2} $year^{-1}$ for the individual PAHs associated with the particulate phase (c = 0.01-0.02 ng m^{-3}; Table 2b), such as BAP, and 0.5 and 0.3 μg m^{-2} $year^{-1}$, respectively, for the total flux of particulate phase PAHs in the ISS and SEM in summer, respectively. The flux will be higher in winter, because of the seasonality of the emissions.

Three gas-particle partitioning models were tested and found to underpredict the particulate mass fraction in most of the samples (four PAHs i.e., BAA, TPH, CHR and BBF). Although input parameters were incomplete these results confirm the earlier insight that additional

processes on the molecular level need to be included, beyond adsorption (Junge-Pankow model) and absorption in OM (K_{oa} models), namely both adsorption and absorption (Lohmann and Lammel, 2004) or even a complete description of molecular interactions between sorbate and PM matrix (Goss and Schwarzenbach, 2001).

Simulations with a non-steady state 2-box model confirm the hypothesis that seasonal depositional input of RET from biomass burning into the surface waters during summer is followed by a period of flux reversal. The volatilisation flux is smaller in magnitude than the net-deposition flux during the previous months, but correspondingly, i.e. higher after intense fire seasons. Future negative emission trends or interannual variability of regional sources may trigger the sea to become a secondary PAH source through reversal of diffusive air-sea exchange. For the wood burning marker RET it is found that the secondary source became significant in recent years: While the flux of secondary RET emissions (from surface seawaters) in the study area was 1.0 μg m^{-2} $year^{-1}$ (mean of years 2005-2010,_UEPS), the primary sources amounted to 3.1 μg m^{-2} $year^{-1}$. Because of non-diffusive emission from the sea surface, such as aerosol suspension from sea spray and bubble bursting (Woolf, 1997; Qureshi et al., 2009; Albert et al., 2012), the true volatilisation may have exceeded the diffusive flux significantly.

Acknowledgements

We thank the crew of RV Urania for scientific support during the cruise, and Giorgos Kouvarakis and Nikolaos Mihalopoulos, University of Crete, Franz Meixner, MPIC, and Manolios Tsapakis, HCMR Gournes-Pediados, for discussion and providing meteorological data. This research was supported by the Granting Agency of the Czech Republic (GACR project No. P503/11/1230), by the European Commission (European Structural Funds project No. CZ.1.05/2.1.00/01.0001, CETOCOEN) and has been co-funded from the European Social Fund and the state budget of the Czech Republic.

References

Akyüz, M., Çabuk, H.: Gas-particle partitioning and seasonal variation of polycyclic aromatic hydrocarbons in the atmosphere of Zonguldak, Turkey. Sci. Total Environ., 2010, 408, 5550-5558.

Albert, M.F.M.A., Schaap, M., Manders, A.M.M., Scannell, C., O'Dowd, C.D., de Leeuw, G.: Uncertainties in the determination of global sub-micron marine organic matter emissions, Atmos. Environ., 2012, 57, 289-300.

Balasubramanian, R., He, J.: Fate and transfer of persistent organic pollutants in a multimedia environment. In: Zereini, F., Wiseman, C.L.S. (eds) Urban airborne particulate matter: origins, chemistry, fate and health impacts. Springer, Heidelberg, pp. 277-307, 2010.

Berrojalbiz, N., Dachs, J., Ojeda, M.J., Valle, M.C., Castro Jiménez, J., Wollgast, J., Ghiani, M., Hanke, G., Zaldivar, J.M.: Biogeochemical and physical controls on concentrations of polycyclic aromatic hydrocarbons in water and plankton of the Mediterranean and Black Seas, Glob. Biogeochem. Cycles, 2011, 25, GB4003.

Bidleman, T.F., McConnell, L.L.: A review of field experiments to determine air–water gas-exchange of persistent organic pollutants. Sci. Total Environ., 1995, 159, 101-107.

Bruhn, R., Lakaschus, S., McLachlan, M.S.: Air/sea gas exchange of PCBs in the southern Baltic sea. Atmos. Environ., 2003, 37, 3445–3454.

Castro-Jiménez, J., Berrojalbiz, N., Wollgast, J., Dachs, J.: Polycyclic aromatic hydrocarbons (PAHs) in the Mediterranean Sea: Atmospheric occurrence, deposition and decoupling with settling fluxes in the water column. Environ. Pollut., 2012, 166, 40-47.

Chrysikou, L.P., Gemenetzis, P.G., Samara, C.A.: Wintertime size distributions of polycyclic aromatic hydrocarbons (PAH). polychlorinated biphenyls (PCB) and organochlorine pesticides (OCPs) in the urban environment: Street- vs. rooftop-level measurements. Atmos. Environ., 2009, 43, 290-300.

Dachs, J., Bayona, J.M., Raoux, C., Albaiges, J.: Spatial, vertical distribution and budget of polycyclic aromatic hydrocarbons in the western Mediterranean seawater. Environ. Sci. Technol., 1997, 31, 682-688.

Dvorská, A., Lammel, G., Klánová, J.: Use of diagnostic ratios for studying source apportionment and reactivity of ambient polycyclic aromatic hydrocarbons over central Europe. Atmos. Environ., 2011, 45, 420-427.

Eckhardt, S., Breivik, K., Manø, S., Stohl, A.: Record high peaks in PCB concentrations in the Arctic atmosphere due to long-range transport of biomass burning emissions, Atmos. Chem. Phys., 2007, 7, 4527–4536.

Finizio, A., Mackay, D., Bidleman, T.F., Harner, T.: Octanol-air partition coefficient as a predictor of partitioning of semi-volatile organic chemicals to aerosols. Atmos. Environ., 1997, 31, 2289-2296.

Franklin, J., Atkinson, R., Howard, P.H., Orlando, J.J., Seigneur, C., Wallington, T.J., Zetzsch, C.: Quantitative determination of persistence in air. In: Criteria for persistence and long-range transport of chemicals in the environment (Klečka, G., Boethling, B., Franklin, J., Grady, L., Graham, D., Howard, P.H., Kannan, K., Larson, R.J., Mackay, D., Muir, D., van de Meent, D., eds.), SETAC Press, Pensacola, USA, pp. 7-62, 2000.

Galarneau, E., Bidleman, T.F., Blanchard, P.: Modelling the temperature-induced blow-off and blow-on artefacts in filter-sorbent measurements of semivolatile substances. Atmos. Environ., 2006, 40, 4258-4268.

Goss, K.U., Schwarzenbach, R.P.: Linear free energy relationships used to evaluate equilibrium partitioning of organic compounds. Environ. Sci. Technol., 2001, 35, 1–9.

Greenfield, B.K., Davis, J.A.: A PAH fate model for San Francisco Bay, Chemosphere, 2005, 6, 515-530.

Guitart, C., Garcá-Flor, N., Miquel, J.C., Fowler, S.W., Albaíges, J.: Effect of accumulation PAHs in the sea surface microlayer on their coastal air-sea exchange, J. Mar. Systems, 2010, 79, 210-217

Harner, T., Bidleman, T.F.: Octanol–air partition coefficient for describing particle-gas partitioning of aromatic compounds in urban air. Environ Sci Technol,, 1998, 32, 1494 – 1502.

Hoff, E.M., Brice, K.A., Halsall, C.J.: Non-linearities in the slope of Clausius-Clapeyron plots for semivolatile organic compounds. Environ. Sci. Technol., 1998, 32, 1793–1798.

Jaenicke, R.: Aerosol physics and chemistry. In: Numerical Data and Functional Relationships in Science and Technology, ed. G. Fischer, vol. 4, pp. 391-457, Springer, Berlin, 1988.

Kaiser, J.W., Heil, A., Andreae, M.O., Benedetti, A., Chubarova, N., Jones, L., Morcrette, J.J., Razinger, M., Schultz, M.G., Suttie, M., van der Werf, G.R.: Biomass burning

emissions estimated with a global fire assimilation system based on observed fire radiative power. Biogeosci., 2012, 9, 527-554.

Karickhoff, S.W.: Semiempirical estimation of sorption of hydrophobic pollutants on natural sediments and soils. Chemosphere, 1981, 10, 833-849.

Kavouras, I.G., Stephanou, E.G.: Particle size distribution of organic primary and secondary aerosol constituents in urban, background marine, and forest atmosphere. J. Geophys. Res., 2002, 107, 4069.

Keyte, I.J., Harrison, R.M., Lammel, G.: Chemical reactivity and long-range transport potential of polycyclic aromatic hydrocarbons – a review, Chem. Soc. Rev., 2013, 42, 9333-9391.

Kiss, G., Varga-Puchony, Z., Rohrbacher, G., Hlavay, J.: Distribution of polycyclic aromatic hydrocarbons on atmospheric aerosol particles of different sizes, Atmos. Res., 1998, 46, 253-261.

Klánová, J., Čupr, P., Kohoutek, J, Harner, T., 2008. Assessing the influence of meteorological parameters on the performance of polyurethane foam-based passive air samplers, Environ. Sci. Technol. 42, 550-555.

Lammel, G.: Effects of time-averaging climate parameters on predicted multicompartmental fate of pesticides and POPs. Environ. Pollut., 2004, 128, 291-302.

Lammel, G., Sehili, A.M., Bond, T.C., Feichter, J., Grassl, H.: Gas/particle partitioning and global distribution of polycyclic aromatic hydrocarbons – a modelling approach. Chemosphere, 2009a, 76, 98-106.

Lammel, G., Klánová, J., Kohoutek, J., Prokeš, R., Ries, L., Stohl, A.: Observation and origin of organochlorine pesticides, polychlorinated biphenyls and polycyclic aromatic hydrocarbons in the free troposphere over central Europe. Environ. Pollut., 2009b, 157, 3264-3271.

Lammel G., Klánová J., Ilić P., Kohoutek J., Gasić B., Kovacić I., Lakić N., Radić R.: Polycyclic aromatic hydrocarbons on small spatial and temporal scales – I. Levels and variabilities, Atmos. Environ., 2010a, 44, 5015-5021.

Lammel, G., Klánová, J., Ilić, P., Kohoutek, J., Gasić, B., Kovacić, I., Škrdlíková, L.: Polycyclic aromatic hydrocarbons on small spatial and temporal scales – II. Mass size distributions and gas-particle partitioning, Atmos. Environ., 2010b, 44, 5022-5027.

572 Lammel, G., Novák, J., Landlová, L., Dvorská, A., Klánová, J., Čupr, P., Kohoutek, J.,
573 Reimer, E., Škrdlíková, L.: Sources and distributions of polycyclic aromatic
574 hydrocarbons and toxicity of polluted atmosphere aerosols. In: Urban Airborne
575 Particulate Matter: Origins. Chemistry. Fate and Health Impacts (Zereini. F., Wiseman.
576 C.L.S., eds.), Springer, Berlin, pp. 39-62, 2010c.
577 Lei, Y.D., Chankalal, R., Chan, A., Wania, F.: Supercooled liquid vapor pressures of the
578 polycyclic aromatic hydrocarbons. J. Chem. Eng. Data, 2002, 47, 801–806.
579 Lim, L., Wurl, O., Karuppiah, S., Obbard, J.P.: Atmospheric wet deposition of PAHs to the
580 sea-surface microlayer, Mar. Poll. Bull., 2007, 54, 1212-1219.
581 Lipiatou, E., Saliot, A.: Fluxes and transport of anthropogenic and natural polycyclic
582 aromatic-hydrocarbons in the western Mediterranean Sea. Mar. Chem., 1991, 32, 51-71.
583 Lipiatou, E., Tolosa, I., Simó, R., Bouloubassi, I., Dachs, J., Marti, S., Sicre, M.A., Bayona,
584 J.M.,. Grimalt, J.O., Saliott, A., Albaiges J.: Mass budget and dynamics of polycyclic
585 aromatic hydrocarbons in the Mediterranean Sea, Deep Sea Res. II, 1997, 44, 881-905.
586 Liss, P.S., Slater, P.G.: Flux of gases across air–sea interface. Nature, 1974, 247, 181-184.
587 Lohmann, R., Lammel G.: Adsorptive and absorptive contributions to the gas particle
588 partitioning of polycyclic aromatic hydrocarbons: State of knowledge and recommended
589 parameterization for modelling. Environ. Sci. Technol., 2004, 38, 3793-3803.
590 Lohmann, R., Dapsis, M., Morgan, E.J., Dekany, E., Luey, P.J.: Determining airwater
591 exchange spatial and temporal trends of freely dissolved PAHs in an urban estuary using
592 passive polyethylene samplers. Environ. Sci. Technol., 2011, 45, 2655-2662.
593 Lüers, F., ten Hulscher, T.E.M.: Temperature effect on the partitioning of polycyclic aromatic
594 hydrocarbons between natural organic carbon and water. Chemosphere, 1996, 33, 643-
595 657.
596 Ma, Y.G., Lei, Y.D., Xiao, H., Wania, F., Wang, W.H.: Critical review and recommended
597 values for the physical-chemical property data of 15 polycyclic aromatic hydrocarbons at
598 25°C. J. Chem. Eng. Data, 2010, 55, 819-825
599 Mai, C.: Atmospheric deposition of organic contaminants into the North Sea and the western
600 Baltic Sea, PhD thesis, University of Hamburg, Hamburg, Germany, 444 pp., URL:
601 http://www.chemie.uni-hamburg.de/bibliothek/diss2012_/DissertationMai.pdf, 2012.

602 Mandalakis, M., Tsapakis, M., Tsoga, A., Stephanou, E.G.: Gas–particle concentrations and
603 distribution of aliphatic hydrocarbons, PAHs, PCBs and PCDD/Fs in the atmosphere of
604 Athens (Greece). Atmos. Environ., 2002, 36, 4023-4035.
605 Masclet, P., Pistikopoulos, P., Beyne, S., Mouvier, G. : Long range transport and gas/particle
606 distribution of polycyclic aromatic hydrocarbons at a remote site in the Mediterranean
607 Sea, Atmos. Environ., 1988, 22, 639–650.
608 Pankow, J.F.: Review and comparative analysis of the the theory of partitioning between the
609 gas and aerosol particulate phases in the atmosphere. Atmos. Environ., 1987, 21, 2275-
610 2283.
611 Pankow, J.F., Bidleman, T.F.: Interdependence of the slopes and intercepts from log-log
612 correlations of measured gas-particle partitioning and vapor pressure. I. Theory and
613 analysis of available data. Atmos. Environ., 1992, 26A, 1071-1080.
614 Pujo-Pay, M., Conan, P., Oriol, L., Cornet-Barthaux, V., Falco, C., Ghiglione, J.F., Goyet, C.,
615 Moutin, T., Prieur, L.: Integrated survey of elemental stoichiometry (C, N, P) from the
616 western to eastern Mediterranean Sea. Biogeosci., 2011, 8, 883-899.
617 Putaud, J.P., Raes, F., van Dingenen, R., Brüggemann, E., Facchini, M.C., Decesari, S.,
618 Fuzzi, S., Gehrig, R., Hüglin, C., Laj, P., Lorbeer, G., Maenhaut, W., Mihalopoulos, N.,
619 Müller, K., Querol, X., Rodriguez, S., Schneider, J., Spindler, G., ten Brink, H., Tørseth,
620 K., Wiedensohler, A.: A European aerosol phenomenology-2: chemical characteristics of
621 particulate matter at kerbside, urban, rural and background sites in Europe. Atmos.
622 Environ., 2004, 38, 2579–2595.
623 Qureshi, A., MacLeod, M., Hungerbühler, K.: Modeling aerosol suspension from soils and
624 oceans as sources of micropollutants to air. Chemosphere, 2009, 77, 495-500.
625 Ramdahl, T.: Retene — a molecular marker of wood combustion in ambient air. Nature,
626 1983, 306, 580 - 582.
627 Rowe, C.L., Mitchelmore, C.L., Baker, J.E.: Lack of biological effects of water
628 accommodated fractions of chemically-and physically-dispersed oil on molecular,
629 physiological, and behavioral traits of juvenile snapping turtles following embryonic
630 exposure. Sci. Total Environ., 2009, 407, 5344-5355.

631 Schmidl, C., Bauer, H., Dattler, A., Hitzenberger, R., Weissenböck, G.: Chemical
632 characterisation of particle emissions from burning leaves. Atmos. Environ., 2008, 42,
633 9070–9079.
634 Schnelle, J., Jänsch, J., Wolf, K., Gebefügi, I., Kettrup, A.: Particle size dependent
635 concentrations of polycyclic aromatic hydrocarbons (PAH) in the outdoor air.
636 Chemosphere, 1995, 31, 3119-3127.
637 Schwarzenbach, R.P., Gschwend, P.M. Imboden, D.M.: Environmental Organic Chemistry.
638 2nd ed., Wiley, Hoboken, USA, 2003.
639 Spindler, G., Gnauk, T., Grüner, A., Iinuma, Y., Müller, K., Scheinhardt, S., Herrmann, H.:
640 Site-segregated characterization of PM_{10} at the EMEP site Melpitz (Germany) using a
641 five-stage impactor: a six year study. J. Atmos. Chem., 2012, 69, 127-157.
642 Stohl, A., Hitzenberger, M., Wotawa, G.: Validation of the Lagrangian particle dispersion
643 model FLEXPART against large scale tracer experiments. Atmos. Environ., 1998, 32,
644 4245-4264.
645 Stohl, A., Forster, C., Eckhardt, S., Spichtinger, N., Huntrieser, H., Heland, J., Schlager,
646 H.,Wilhelm, S., Arnold, F., Cooper, O.: A backward modeling study of intercontinental
647 pollution transport using aircraft measurements. J. Geophys. Res., 2003, 108, 4370,
648 doi:10.1029/2002jd002862.
649 Stohl, A., Forster, C., Frank, A., Seibert, P., Wotawa, G.: Technical Note: The Lagrangian
650 particle dispersion model FLEXPART version 6.2. Atmos. Chem. Phys., 2005, 5, 2461-
651 2474.
652 Tsapakis, M., Stephanou, E.G.: Collection of gas and particle semi-volatile organic
653 compounds: Use of an oxidant denuder to minimize polycyclic aromatic hydrocarbons
654 degradation during high-volume air sampling. Atmos. Environ., 2003, 37, 4935-4944.
655 Tsapakis, M., Stephanou, E.G.: Polycyclic aromatic hydrocarbons in the atmosphere of the
656 Eastern Mediterranean. Environ. Sci. Technol., 2005a, 39, 6584-6590.
657 Tsapakis, M., Stephanou, E.G.: Occurrence of gaseous and particulate polycyclic aromatic
658 hydrocarbons in the urban atmosphere: study of sources and ambient temperature effect
659 on the gas/particle concentration and distribution. Environ. Poll., 2005b, 133, 147-156.

Tsapakis, M., Stephanou, E.G., Karakassis, I.: Evaluation of atmospheric transport as a non-point source of polycyclic aromatic hydrocarbons in marine sediments of the Eastern Mediterranean, Mar. Chem., 2003, 80, 283-298.

Tsapakis, M., Apostolaki, M., Eisenreich, S., Stephanou, E.G.: Atmospheric deposition and marine sedimentation fluxes of polycyclic aromatic hydrocarbons in the Eastern Mediterranean Basin, Environ. Sci. Technol., 2006, 40, 4922-4927.

Woolf, D.K.: Bubbles and their role in gas exchange, in: Sea Surface and Global Change (Liss, P.S., Duce, R.A., eds.), Cambridge University Press, Cambridge, UK, pp. 173-206, 1997.

Zhong, G., Xie, Z., Möller, A., Halsall, C., Caba, A., Sturm, R., Tang, J., Zhang, G., Ebinghaus, R.: Currently used pesticides, hexachlorobenzene and hexachlorocyclohexanes in the air and seawater of the German Bight (North Sea). Environ. Chem., 2012, 9, 405-414.